

# Shrinking Magnetic Vortices in $V_3Si$ Due to Delocalized Quasiparticle Core States: Confirmation of the Microscopic Theory for Interacting Vortices

J.E. Sonier<sup>1,2</sup>, F.D. Callaghan<sup>1</sup>, R.I. Miller<sup>3</sup>, E. Boaknin<sup>4</sup>, L. Taillefer<sup>2,5</sup>,

R.F. Kiefl<sup>2,6</sup>, J.H. Brewer<sup>2,6</sup>, K.F. Poon<sup>1</sup> and J.D. Brewer<sup>1</sup>

<sup>1</sup>*Department of Physics, Simon Fraser University, Burnaby, British Columbia V5A 1S6, Canada*

<sup>2</sup>*Canadian Institute for Advanced Research, Toronto, Ontario, Canada*

<sup>3</sup>*Department of Physics & Astronomy, University of Pennsylvania, Philadelphia, PA 19104*

<sup>4</sup>*Department of Applied Physics, Yale University, New Haven, CT 06520-8284*

<sup>5</sup>*Département de Physique, Université de Sherbrooke, Québec J1K 2R1, Canada*

<sup>6</sup>*Department of Physics and Astronomy, University of British Columbia, Vancouver, British Columbia V6T 1Z1, Canada*

(Dated: September 26, 2018)

We report muon spin rotation measurements on the conventional type-II superconductor  $V_3Si$  that provide clear evidence for changes to the inner structure of a vortex due to the delocalization of bound quasiparticle core states. The experimental findings described here confirm a key prediction of recent microscopic theories describing interacting vortices. The effects of vortex-vortex interactions on the magnetic and electronic structure of the vortex state are of crucial importance to the interpretation of experiments on both conventional and exotic superconductors in an applied magnetic field.

PACS numbers: 74.20.Fg, 74.25.Qt, 74.70.Ad, 76.75.+i

In 1964, a breakthrough paper by Caroli, de Gennes and Matricon [1] showed that in the framework of the microscopic theory, quasiparticles (QPs) bound to an *isolated* vortex of a conventional *s*-wave type-II superconductor occupy discrete energy levels. Twenty-five years later, localized vortex core states were observed for the first time in  $NbSe_2$  by scanning tunneling microscopy (STM) [2]. Our understanding of the vortex state in type-II superconductors has accordingly progressed from Abrikosov's initial prediction [3] based on the macroscopic Ginzburg-Landau (GL) theory [4], to current theories describing the electronic structure of magnetic vortices on a microscopic level. However, it is only in recent years that predictions have emerged from the microscopic theory on the effects of *vortex-vortex interactions*. In analogy with bringing atoms close together to form a conducting solid, increasing the vortex density by applying a stronger magnetic field  $H$  enhances the overlap of bound state wave functions of neighboring vortices, resulting in the formation of energy bands that allow the intervortex transfer of QPs [5, 6, 7, 8]. This is expected to strongly influence experiments on conventional superconductors that are sensitive to quasiparticle excitations, such as specific heat and thermal transport, and to have profound effects on the magnetic structure of the vortex state. However, understanding the potential interplay between vortices and quasiparticles is also of crucial importance in the study of high-temperature superconductors. In these and other exotic superconductors, comparatively little is known about the structure of the vortex state and its effect on experiments in large magnetic fields. It is therefore essential to have a solid understanding of the behavior of interacting vortices in conventional superconductors, and to establish the connections with quasiparticle properties.

The effect of delocalized QP core states on the spatial variation of the pair potential  $\Delta(r)$  at a vortex site

has been considered in the framework of the quasiclassical Eilenberger theory [7, 8, 9]. These calculations show that the effect of the intervortex transfer of QPs on  $\Delta(r)$  leads to a reduction of the size of the vortex cores with increasing  $H$ . Such shrinking of the vortex cores has in fact been observed by muon spin rotation ( $\mu$ SR) [10, 11, 12, 13, 14, 15, 16] and STM [17], and proposed as a possible explanation for the anomalous low-field behavior observed of the specific heat in conventional superconductors [18, 19]. However, experimentally there has been inadequate evidence in support of a causal relationship between the size of the vortex cores and the delocalization of bound QP core states.

An important finding has come by way of recent low-temperature thermal conductivity measurements, which are sensitive only to extended or delocalized electronic excitations. These studies have revealed the existence of highly delocalized QPs down to low magnetic fields in the vortex state of  $LuNi_2B_2C$  [20],  $YBa_2Cu_3O_{6.9}$  [21],  $NbSe_2$  [22] and  $MgB_2$  [23]. In the extreme gap anisotropy superconductors  $LuNi_2B_2C$  and  $YBa_2Cu_3O_{6.9}$ , the dominant contribution to the thermal conductivity is believed to be a field-induced Doppler shift of the QP spectrum outside the vortex cores [24]. Most surprising are the results for  $NbSe_2$ , long believed to be representative of a simple conventional *s*-wave superconductor. The high degree of QP delocalization in  $NbSe_2$  appears to arise from two-gap superconductivity [22], as is the case for  $MgB_2$  [23]. In these superconductors, the heat at low fields is carried by the QP excitations associated with the smaller of the two energy gaps. This smaller gap is a possible source of the very large low-field value of the core size observed in  $NbSe_2$  by  $\mu$ SR [10] and in  $MgB_2$  by STM [25]. On the other hand, the large core size observed at low fields in borocarbide [15, 16] and cuprate [11, 12, 13] superconductors is not completely understood.

The conventional superconductors  $V_3Si$  and Nb pro-

vide a unique opportunity to experimentally observe the effects of intervortex QP transfer on the inner structure of a vortex. In contrast to the abovementioned superconductors, thermal conductivity measurements [22, 26] reveal no appreciable delocalization of QP states at low  $H$  — as expected when the vortices are nearly isolated.  $V_3Si$  is particularly suitable, since it has a simple cubic crystal structure, a relatively high superconducting transition temperature ( $T_c = 17$  K) and a large upper critical field ( $H_{c2} \approx 185$  kOe). To determine the size of the vortex cores we measured the internal magnetic field distribution in  $V_3Si$  by  $\mu$ SR at the Tri-University Meson Facility (TRIUMF), Vancouver, Canada. The experiment was performed by implanting spin-polarized muons, which stop randomly in the sample on the length scale ( $\sim 10^2$ - $10^3$  Å) of the vortex lattice (VL). The magnetic moment of the muon precesses about the local magnetic field  $B$  with a Larmor frequency given by  $\nu = \gamma_\mu B$ , where  $\gamma_\mu = 0.0852 \mu s^{-1} G^{-1}$  is the gyromagnetic ratio of the muon. The spatial distribution of  $B$  is determined by measuring the time evolution of the muon spin polarization via the anisotropic distribution of decay positrons [27].

Small-angle neutron scattering [28] and recent STM [29] images of  $V_3Si$  show that for a field applied along the fourfold [001] axis, the VL undergoes a transition from hexagonal to square symmetry. Kogan *et al.* [30] have developed a phenomenological London model that attributes this transition to nonlocality of the relation between the supercurrent density  $\mathbf{j}(\mathbf{r})$  and the vector potential  $\mathbf{A}$  in a region around the vortex core. This establishes a connection between the vortex structure and the anisotropy of the Fermi surface, which in  $V_3Si$  produces fourfold symmetry near the vortex cores. We note that a more general model has recently been developed for fourfold symmetric superconductors, which incorporates the effects of both Fermi surface and gap anisotropy on the vortex structure [31]. At fields below 7.5 kOe where the intervortex spacing is large, the isotropic magnetic repulsion of vortices yields a hexagonal lattice. With increasing field there is an increased overlap of the fourfold symmetric regions of the individual vortices, and the VL evolves into a square at 40 kOe.

The Kogan model uses an arbitrary cutoff factor to overcome the logarithmic divergence of the internal magnetic field  $B(r)$  at the vortex sites. We find that the  $\mu$ SR data are fit much better using a GL analog of the Kogan model, which properly accounts for the finite size of the vortex cores [32]. The spatial profile of the periodic local magnetic field in the GL formalism is given by

$$B(r) = B_0(1 - b^4) \sum_{\mathbf{G}} \frac{e^{-i\mathbf{G}\cdot\mathbf{r}} u K_1(u)}{\lambda^2 G^2 + \lambda^4 (n_{xxyy} G^4 + d G_x^2 G_y^2)}. \quad (1)$$

Here  $b = B/B_{c2}$  is the reduced field,  $B_0$  is the average internal field,  $\mathbf{G}$  are the reciprocal lattice vectors,  $K_1(u)$  is a modified Bessel function,  $u^2 = 2\xi^2 G^2(1 + b^2)[1 - 2b(1 - b)^2]$ ,  $\xi$  is the GL coherence length, and  $n_{xxyy}$  and

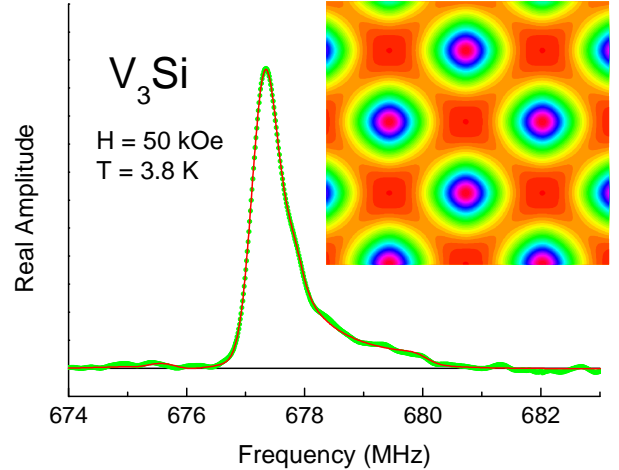


FIG. 1: Fourier transform (FT) of the measured muon spin precession signal (green circles) in  $V_3Si$  at  $T = 3.8$  K and  $H = 50$  kOe. The FT provides an approximate illustration of the internal magnetic field distribution, but is broadened by the apodization procedure used to smooth out the ringing effects of the finite time window (0-3  $\mu s$ ) and the noise from reduced counts at later times. Additional broadening due to VL disorder and nuclear magnetic dipoles is accounted for by a Gaussian broadening width of  $\sigma \approx 1.0 \mu s^{-1}$ . The solid red curve is the FT of the fit in the time domain, assuming the field profile  $B(r)$  given by Eq. (1). The inset is a contour plot of the function  $B(r)$  obtained from the fit.

$d$  are dimensionless parameters arising from the nonlocal corrections. The quartic  $n_{xxyy}$  term is an isotropic correction, whereas the biquadratic  $d$  term controls the fourfold anisotropy.

Figure 1 shows Fourier transforms of both the measured muon-spin precession signal and the fit to the data in the time domain at 50 kOe applied parallel to [001]. In agreement with the imaging experiments, we obtained excellent fits to a square and hexagonal VL above 40 kOe and below 7.5 kOe, respectively, and to a rhombic unit cell with an apex angle  $\beta \approx 60^\circ - 90^\circ$  at intermediate fields. These fits and those to Kogan's model also yielded the following results: (i) For all  $H$ ,  $n_{xxyy} \approx 0$ . This is consistent with an analogous model developed by Affleck, Franz and Amin [33], who found that the quartic correction makes a negligible contribution. (ii) Below 7.5 kOe, excellent fits were obtained with  $d = 0$ . This indicates that the VL is not strongly tied to the underlying crystal lattice, as was determined by STM. (iii) Above 7.5 kOe, the orientation of the vortex cores determined by our analysis (see Fig. 1 inset) is that which is expected for close packing of square vortices.

The field dependence of  $\lambda$ ,  $\xi$ ,  $d$  and  $\beta$  are shown in Fig. 2. At low fields where the lattice is hexagonal,  $\lambda \approx 1060$  Å and  $\xi \approx 42$  Å, which are consistent with previously determined values of these parameters. Above 7.5 kOe there is a slight nonphysical increase in the fit-

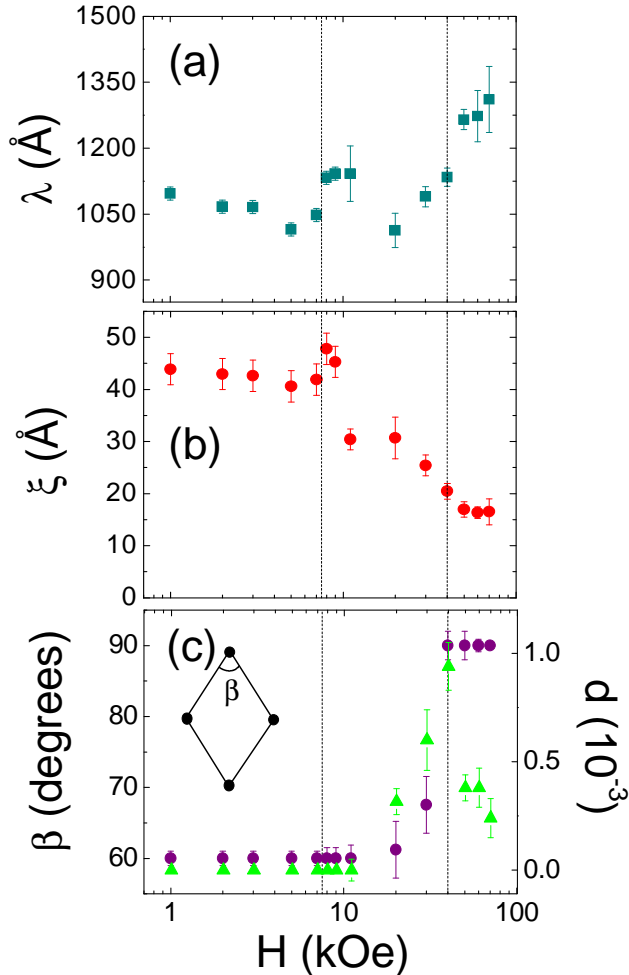


FIG. 2: The magnetic field dependence of the fit parameters at  $T = 3.8$  K. (a) The magnetic penetration depth  $\lambda$ . (b) The coherence length  $\xi$ . (c) The apex angle  $\beta$  (purple circles) and the anisotropy parameter  $d$  (green triangles). The dashed vertical lines indicate the field range over which the VL continuously evolves from hexagonal to square symmetry. At fields immediately above 7.5 kOe,  $d$  and  $\beta$  are poorly determined, because the VL is only slightly distorted from hexagonal symmetry.

ted values of  $\lambda$  and  $\xi$ , reflecting the beginning of the gradual transition to a square VL. At higher fields  $\xi$  decreases, and continues to do so when the VL completes its transition to a square at 40 kOe.

Gygi and Schlüter [34] have shown that the pair potential  $\Delta(r)$ , which in general is a numerical function, varies on two length scales,  $\xi_1$  and  $\xi_2$ . The first is defined from the slope of  $\Delta(r)$  near the center of the vortex core

$$\xi_1 = \Delta_0 / \lim_{r \rightarrow 0} \frac{\Delta(r)}{r} \quad (2)$$

( $\Delta_0$  is the BCS superconducting energy gap), whereas  $\xi_2$  is the length scale over which  $\Delta(r)$  rises to its asymptotic

value  $\Delta_0$ . It is important to note that while at low temperatures  $\xi_2$  is close to the value of the coherence length derived from  $H_{c2}$  (*i.e.*  $\sim 42$  Å),  $\xi_1$  is considerably shorter [see Fig. 3(b)]. Thus, we can understand the reduction of  $\xi$  above 7.5 kOe as a rapid variation of  $\Delta(r)$  at the vortex center, and not an increase of  $H_{c2}$ . Theoretically, the rapid increase of  $\Delta(r)$  near  $r = 0$  is accompanied by a similar rise of the supercurrent density  $j(r)$  in the same region [7, 8, 34]. Consequently, we can define an effective vortex-core size  $r_0$  as the distance from the core centre ( $r = 0$ ) to the location where  $j(r)$  reaches its maximum value, measured along the line connecting nearest-neighbor vortices. Solutions of the microscopic theory show that  $\xi_1$  and  $r_0$  exhibit the same qualitative behavior as functions of  $H$  and  $T$ . From previous  $\mu$ SR studies of the Kramer-Pesch effect, it is known that the fitted value of  $\xi$  in Eq. (1) and  $r_0$  exhibit similar behavior, and hence  $\xi$  reflects a particular sensitivity to  $\xi_1$ . The parameter  $r_0$  can be obtained in a nearly model-independent way using the Maxwell relation,  $j(r) = |\nabla \times \mathbf{B}(\mathbf{r})|$ , where  $B(r)$  is obtained from fitting the  $\mu$ SR time spectrum. Because  $r_0$  is not a fit parameter, the details of the theoretical model for  $B(r)$  are not very important in this procedure. What is essential is that the model for  $B(r)$  yields excellent fits, as was the case using Eq. (1).

In Fig. 3(a) we compare the field dependence of  $r_0$  in  $V_3Si$  to the electronic thermal conductivity  $\kappa_e$  measured previously [22]. For the first time we see the expected field dependence of the core size in a single-gap conventional  $s$ -wave superconductor. In contrast to  $NbSe_2$  [10] and  $MgB_2$  [25], the low-field value of  $r_0$  is consistent with the coherence length calculated from  $H_{c2}$ . At low fields, where only a modest overlap of the QP core states of neighboring vortices is expected, both  $r_0$  and  $\kappa_e$  exhibit a weak dependence on  $H$ . The change in  $r_0$  over this range of  $H$  is primarily due to the superposition of the  $j(r)$  profiles of nearest-neighbor vortices. This is indicated by the green circles in Fig. 3. Above 7.5 kOe the core size shrinks more rapidly than that expected from the superposition of  $j(r)$  profiles, and is accompanied by a simultaneous increase in the electronic thermal conductivity. Together these observations signify a change in the slope of  $\Delta(r)$  at the vortex center, due to an increased overlap of the bound state wave functions of adjacent vortices. As shown in Fig. 3(a), the transformation to a square vortex lattice begins at the field where the delocalization of QPs becomes significant. In other words, it is the increased strength of the vortex-vortex interactions that drives the symmetry change of the lattice to reflect the fourfold symmetry of the individual vortices.

The experimental results presented here for  $V_3Si$  confirm one of the key predictions of theoretical works that advocate the importance of intervortex QP transfer to the detailed structure of the VL. This important detail should be a consideration in the interpretation of any experiment on a type-II superconductor in an applied magnetic field.

We thank Tetsuo Fukase for providing us with the sam-

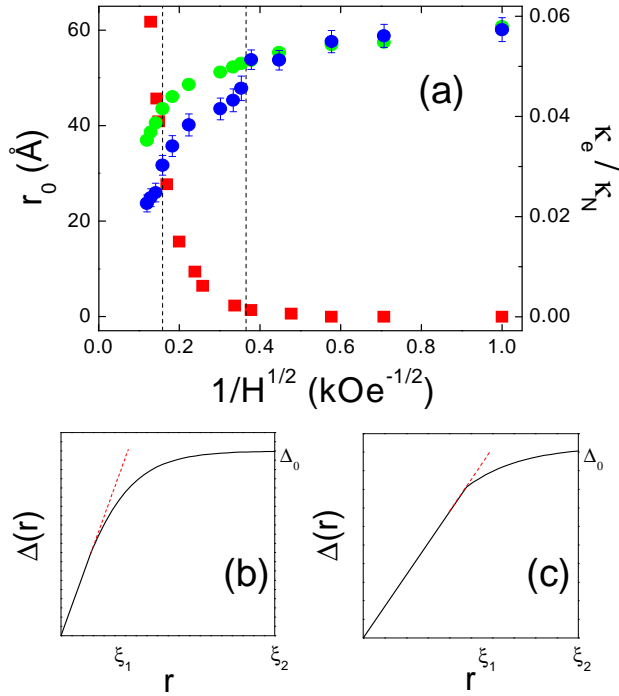


FIG. 3: (a) The magnetic field dependence of the vortex core size  $r_0$  measured by  $\mu$ SR (blue circles) at  $T = 3.8$  K, and the electronic thermal conductivity  $\kappa_e/T$  (red squares) from Ref. [22] extrapolated to  $T \rightarrow 0$  (and normalized to the value  $\kappa_N/T$  at  $H_{c2}$ ). The green circles indicate the reduction of  $r_0$  due to the superposition of  $j(r)$  profiles from individual vortices, calculated assuming the low-field value of  $\xi$ . The data are plotted as a function of  $1/H^{1/2}$ , which is proportional to the intervortex spacing  $L = (\Phi_0/H \sin \beta)^{1/2}$ , where  $\Phi_0$  is the magnetic flux quantum. The dashed vertical lines indicate the field range over which the VL undergoes a continuous hexagonal-square transition. Schematic of the pair potential  $\Delta(r)$  as a function of distance from the vortex core centre at high (b) and low (c) magnetic field.

ple of  $\text{V}_3\text{Si}$ . This work was supported by the Natural Sciences and Engineering Research Council (NSERC) of Canada and the Canadian Institute for Advanced Research (CIAR).

- 
- [1] C. Caroli, P.G. de Gennes, and J. Matricon, Phys. Lett. **9**, 307 (1964).
  - [2] H.F. Hess, R.B. Robinson, R.C. Dynes, J.M. Valles Jr., and J.V. Waszczak, Phys. Rev. Lett. **62**, 214 (1989).
  - [3] A.A. Abrikosov, Soviet Phys. JETP **5**, 1174 (1957).
  - [4] V.L. Ginzburg and L.D. Landau, Zh. Ekserim. i. Teor. Fiz. **20**, 1064 (1950).
  - [5] B. Pöttinger, and U. Klein, Phys. Rev. Lett. **70**, 2806 (1993).
  - [6] S. Dukan and Z. Tesanović, Phys. Rev. B **49**, 13017 (1994); Z. Tesanović and P. Sacramento, Phys. Rev. Lett. **80**, 1521 (1998).
  - [7] M. Ichioka, A. Hasegawa, and K. Machida, Phys. Rev. B **59**, 184 (1999).
  - [8] M. Ichioka, A. Hasegawa, and K. Machida, Phys. Rev. B **59**, 8902 (1999).
  - [9] A.A. Golubov, and U. Hartmann, Phys. Rev. Lett. **72**, 3602 (1994).
  - [10] J.E. Sonier *et al.*, Phys. Rev. Lett. **79**, 1742 (1997).
  - [11] J.E. Sonier *et al.*, Phys. Rev. Lett. **79**, 2875 (1997).
  - [12] J.E. Sonier *et al.*, Phys. Rev. B **59**, 729(R) (1999).
  - [13] J.E. Sonier *et al.*, Phys. Rev. Lett. **83**, 4156 (1999).
  - [14] R. Kadono *et al.*, Phys. Rev. B **63**, 224520 (2001).
  - [15] K. Ohishi *et al.*, Phys. Rev. B **65**, 140505(R) (2002).
  - [16] A.N. Price *et al.*, Phys. Rev. B **65**, 214520 (2002).
  - [17] U. Hartmann, A.A. Golubov, T. Drechsler, M. Yu. Kupriyanov, and C. Heiden, Physica B **194-196**, 387 (1994).
  - [18] J.E. Sonier, M.F. Hundley, J.D. Thompson, and J.W. Brill, Phys. Rev. Lett. **82**, 4914 (1999).
  - [19] M. Nohara, M. Isshiki, F. Sakai, and H. Takagi, J. Phys. Soc. Jpn. **68**, 1078 (1999).
  - [20] E. Boaknin *et al.*, Phys. Rev. Lett. **87**, 237001 (2001).
  - [21] M. Chiao, R.W. Hill, C. Lupien, B. Popic, R. Gagnon,

- and L. Taillefer, Phys. Rev. Lett. **82**, 2943 (1999).
- [22] E. Boaknin *et al.*, Phys. Rev. Lett. **90**, 117003 (2003).
  - [23] A.V. Sologubenko, J. Jun, S.M. Kazakov, J. Karpinski, H.R. Ott, Phys. Rev. B **66**, 014504 (2002).
  - [24] G.E. Volovik, Pis'ma Zh. Eksp. Teor. Fiz. **58**, 457 (1993).
  - [25] M.R. Eskildsen *et al.*, Phys. Rev. Lett. **89**, 187003 (2002).
  - [26] J. Lowell, and J.B. Sousa, J. Low. Temp. Phys. **3**, 65 (1970).
  - [27] J.E. Sonier, J.H. Brewer, and R.F. Kiefl, Rev. Mod. Phys. **72**, 769 (2000).
  - [28] M. Yethiraj, D.K. Christen, D. McK. Paul, P. Miranović, and J.R. Thompson, Phys. Rev. Lett. **82**, 5112 (1999).
  - [29] C.E. Sosolik *et al.*, Phys. Rev. B **68**, 140503(R) (2003).
  - [30] V.G. Kogan, P. Miranović, Lj. Dobrosavljević-Grujić, W.E. Pickett, and D.K. Christen, Phys. Rev. Lett. **79**, 741 (1997).
  - [31] N. Nakai, P. Miranović, M. Ichioka, and K. Machida, Phys. Rev. Lett. **89**, 237004 (2002).
  - [32] A. Yaouanc, P. Dalmas de Réotier, and E.H. Brandt, Phys. Rev. B **55**, 11107 (1997).
  - [33] I. Affleck, M. Franz, and M.H. Amin, Phys. Rev. B **55**, 704(R) (1997).
  - [34] F. Gygi, and M. Schlüter, Phys. Rev. B **43**, 7609 (1991).